Emerging Applications of Multirate Signal Processing and Wavelets in Digital Communications

GREGORY W. WORNELL, MEMBER, IEEE

Invited Paper

Multirate systems and filterbanks have traditionally played an important role in source coding and compression for contemporary communication applications, and many of the key design issues in such applications have been extensively explored. In this paper, we review recent developments on the comparatively less explored role of multirate filterbanks and wavelets in channel coding and modulation for some important classes of channels. Some representative examples of emerging potential applications are described. One involves the use of highly dispersive, broadband multirate systems for wireless multiuser communication in the presence of fading due to time-varying multipath. Another is the wavelet-based diversity strategy referred to as "fractal modulation" for use with unpredictable communication links and in broadcast applications with user-selectable quality of service. A final example involves multitone (multicarrier) modulation systems based on multirate filterbanks and fast lapped transforms for use on channels subject to severe intersymbol and narrowband interference. Collectively, these constitute intriguing, interrelated paradigms within an increasingly broad and active area of research.

I. Introduction

A central problem within communication theory concerns how to efficiently transmit information-bearing signals over unreliable channels. Depending on the application, the signals of interest may be continuous-time waveforms or discrete-time sequences, and they may be continuous in amplitude or discrete-valued. Examples include speech, image, and video signals, as well as various kinds of inherently digital data.

The communications problem is frequently partitioned into two subproblems—source coding and channel coding. Shannon's celebrated source-channel separation theorem ensures that for some important classes of channels these problems can be addressed independently without loss of performance [1]. However, even when such partitioning cannot be justified in terms of the separation theorem, the approach is often popular for a variety of other reasons, among which are tractability of system design and robustness of the resulting system to errors in source and channel modeling.

In a variety of respects, the source and channel coding problems can be viewed as duals of one another, and this leads to important relationships between the approaches used to address these problems in practice.

Source coding is concerned with developing a maximally compact (i.e., redundancy-free) representation for the information to be conveyed. Typically, a digital representation is sought, in the form of a discrete-valued sequence such as a bit stream. In many cases, some degree of distortion is allowed in the representation, and in this case, the objective is to develop a maximally compact description of the source subject to a constraint on the maximum allowable distortion [2]. Source coding has been a strong and fruitful application focus for much of the current development of multirate signal processing and wavelet theory [3]–[5].

The channel coding that follows source coding is designed to reintroduce—in a controlled manner—a prescribed level of redundancy back into the source coded stream to mitigate the anticipated effects of the channel, and best performance is achieved when the redundancy is tailored to the specific characteristics of the channel. Although channel coding and modulation applications have received comparatively less attention to date, multirate signal processing and wavelet theory also have an important complementary role to play in this aspect of the communications problem.

This paper considers three classes of important communication channels and examines promising paradigms for exploiting multirate filter bank and wavelet representations

Manuscript received June 1, 1995; revised January 15, 1996. This work has been supported in part by the Advanced Research Projects Agency monitored by ONR under Contract Number N00014-93-1-0686, the National Science Foundation under Grant MIP-9502885, and in part by the Office of Naval Research under Grant N0014-95-1-0834.

The author is with the Department of Electrical Engineering and Computer Science, and the Research Laboratory of Electronics, Massachusetts Institute of Technology, Cambridge, MA 02139 USA.

Publisher Item Identifier S 0018-9219(96)03001-0.

in developing systems for reliable transmission over such channels. It is important to emphasize at the outset that this paper does not attempt a comprehensive survey of the existing literature, which would be an overly ambitious undertaking given the rapid pace at which developments in this emerging area are taking place. Rather, as a more modest goal, the paper focuses on three specific but representative examples of some promising recent developments, and explores their interconnections.

The paper is organized as follows. First, Section II considers the problem of multiuser communication over wireless channels subject to fading due to time-varying multipath propagation. For these channels, we examine a novel multirate modulation scheme referred to as spread-signature code division multiple access (CDMA), which is an effective strategy for combating the effects of fading in such environments. As we will see, interestingly, the multirate systems that arise this application have radically different characteristics than those used in source coding applications. We will also see that spread-signature CDMA can be adapted for use in single-user systems, yielding very efficient implementations of a technique referred to as spread-response precoding.

Next, Section III considers the problem of reliable communication over a class of noisy channels whose key characteristic is that the channel is open for some finite but unknown time interval, during which it has some finite but unknown bandwidth. Such models are useful for a range of wireless and secure communications applications, as well as for broadcast applications in which information is being transmitted to receivers whose front ends have differing bandwidths and processing capabilities. For such channels, a wavelet-based paradigm referred to as "fractal modulation" is examined. This technique, which involves embedding an information stream into a self-similar waveform so that it is present on all time scales, provides a novel and efficient form of diversity for such applications.

Finally, Section IV explores the role of multirate filterbanks and fast lapped transforms in developing efficient multitone modulation schemes for communication over severe intersymbol interference channels and in the presence of strong narrowband interference. As we will see, the resulting schemes, referred to as "lapped multitone modulation," are highly practicable and provide some important advantages over alternative approaches that make them compelling candidates for use in a variety of emerging high-speed data transmission applications.

II. Spread-Signature CDMA

This section focuses on the problem of efficient communication over radio frequency channels. Such channels are used in a host of existing and emerging wireless communications applications ranging from digital mobile radio and indoor personal wireless systems, to digital audio and television broadcasting systems.

In these wireless environments, a transmitted signal generally travels along multiple paths en route to a receiver due to reflections off natural and man-made physical objects, and the results are superimposed at the receiver antenna. This phenomenon is referred to as multipath propagation and can result in attenuation of the signal when the individual paths combine destructively. This attenuation is often severe—fades in signal-to-noise ratio (SNR) of 35 dB or more are not unusual. Depending on the bandwidth of the system, all frequencies may fade in unison, which is termed frequency nonselective or flat fading, or it can be frequency selective. In indoor channels, for example, frequency selective fading is encountered when bandwidths significantly greater than 10 MHz are used. When, in addition, the transmitter and/or receiver are in motion as is typical in cellular telephony applications, this multipath fading is time-varying. This will be the case we consider.

It is also important to note that wireless communication systems can also be subject to other forms of interference. For example, there may be hostile jamming in a military application, or unintentional jamming due to cochannel interference. Depending on its source, this interference may be narrowband or broadband, or impulsive, and in some cases can be the predominant form of noise particularly in multiuser systems.

Diversity techniques are typically used to mitigate the effects of fading during data transmission and can take a variety of forms [6], [7]. For example the use of spectrum in excess of what would ordinarily be required for transmission is a form of *spectral* diversity that is widely exploited in spread-spectrum systems [8], [9]. Likewise, the use of antenna arrays at the transmitters and/or receivers of wireless systems provides valuable *spatial* diversity [6], [7].

This section describes multirate signal processing techniques that can be used either alone or in combination with traditional error correction coding to provide computationally efficient forms of *temporal* diversity in a multiuser environment [10], [11]. The result can be viewed as a CDMA system [9] with some rather special characteristics [12].

A. Channel Model

Although there are a range of other application contexts, for the purposes of illustration we will focus on a cellular multiple-access scenario in which each cell contains a single base station ("cell site") and a number of mobiles ("subscribers"). In such systems, both forward link (base-to-mobile) and reverse link (mobile-to-base) communication is required, but takes place on separate (i.e., noninterfering) channels. Although the systems we examine are applicable for both links, for simplicity of exposition we focus on the reverse link, which is typically more challenging due to the uncoordinated nature of the transmissions.

Consider a single cell of the system, in which there are M users all sharing some total fixed bandwidth. As a reasonable equivalent discrete-time baseband model for the passband communication channel between the mobiles

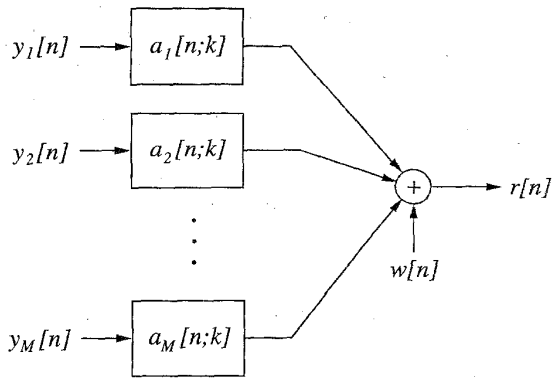

Fig. 1. General multiuser fading channel model, where $a_m[n;k]$ denotes the randomly time-varying linear kernel corresponding to the mth user.

and the base unit, the received signal takes the form

$$r[n] = \sum_{m=0}^{M-1} \sum_{k} a_m[n;k]\, y_m[n-k] + w[n]. \qquad (1)$$

In general, the randomly time-varying kernels[1] $a_m[n;k]$ capture the effects of multipath fading due to both fluctuations in the media and the relative motions of transmitters and receivers in the system, as well as the effects of asynchronism among the users' transmissions. Meanwhile, $w[n]$ captures both receiver noise and any sources of interference not otherwise taken into account. This channel model is depicted in Fig. 1.

When the complex-valued kernels can be modeled as zero-mean and Gaussian, the result is a Rayleigh fading channel [7]. For frequency selective channels, the time-variant frequency response

$$A_m(\omega;n] = \sum_{k} a_m[n;k]e^{-j\omega k}$$

has a magnitude that varies as a function of ω for each n. For frequency nonselective (flat fading) channels, $A_m(\omega;n]$ is independent of ω. Moreover, for reverse link transmission, the kernels of the individual mobile-to-base channels can be modeled as statistically independent provided there is reasonable physical separation between mobiles. Finally, in a typical application the transmitters do not have knowledge of the channel kernels $a_m[n;k]$ or their statistics, while the receiver obtains reliable estimates of these quantities via trained or blind channel identification algorithms.

B. Orthogonal Multiuser Modulation and Spread Signatures

In multiple access systems, a common way to separate users is via a modulation process of the following form. The coded symbol stream of the mth user, which we denote by $x_m[n]$, is modulated onto a unique signature sequence (i.e., discrete-time transmit pulse shape) $h_m[n]$ to produce $y_m[n]$

[1] The kernel $a_m[n;k]$ is the response at time n of the mth user's channel to a unit sample at time $n-k$.

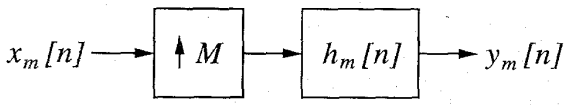

Fig. 2. Modulation of the the mth user's coded symbol stream $x_m[n]$ onto a signature sequence $h_m[n]$ for transmission.

which is transmitted within the total available bandwidth. Fig. 2 depicts this process, which consists of upsampling (i.e., zero insertion) by a factor M, followed by linear time-invariant filtering with the signature sequence, i.e.,

$$y_m[n] = \sum_{k} x_m[k]\, h_m[n-kM]. \qquad (2)$$

A useful mathematical framework for representing sets of signature sequences arises out of multirate system theory. To begin, we first express the signature set as a vector sequence, i.e.,[2]

$$\boldsymbol{h}[n] = \begin{bmatrix} h_1[n] & h_2[n] & \cdots & h_M[n] \end{bmatrix}^T. \qquad (3)$$

When each of the component signatures $h_m[n]$ has only finitely many nonzero values, the signature set is said to have *finite spread.* Specifically, when

$$\boldsymbol{h}[n] = \boldsymbol{0}, \qquad n < 0, n \geq N$$

we say that the signature set has *spread* N.

A natural requirement of such systems is that in the absence of fading, and with perfect synchronism among users, there be no intersymbol interference either within a user's stream or among users. This is equivalent to requiring that the signature sets satisfy certain orthogonality conditions—specifically, that the signature sequences together with all translates by integer multiple of M constitute an orthonormal basis. The orthogonality condition is

$$\sum_{k} \boldsymbol{h}[k-nM]\boldsymbol{h}^T[k-mM] = \delta[n-m]\boldsymbol{I} \qquad (4)$$

where $\boldsymbol{I}$ denotes the identity matrix of appropriate size and where $\delta[n]$ denotes the unit sample, viz.,

$$\delta[n] \triangleq \begin{cases} 1, & n = 0 \\ 0, & \text{otherwise.} \end{cases}$$

The corresponding completeness condition for this orthonormal set can be expressed as

$$\begin{aligned} &\sum_{k} \boldsymbol{h}^T[n-kM]\, \boldsymbol{h}[m-kM] \\ &= \sum_{k,i} h_i[n-kM]\, h_i[m-kM] \\ &= \delta[n-m]. \end{aligned} \qquad (5)$$

Orthogonal modulation is desirable from a variety of perspectives, and simplifies receiver design.

For $M \geq 2$, we can infer from multirate filter bank theory that a rich collection of signature sets satisfy (4) and (5),

[2] The superscript ^{T} denotes transposition.

even when we restrict our attention to signatures with finite-spread. This can be conveniently seen in the frequency domain. To develop frequency domain perspectives, we express the set of Fourier transforms corresponding to (3) in the form

$$\boldsymbol{H}(\omega) = \sum_{n=-\infty}^{+\infty} \boldsymbol{h}[n]\, e^{-j\omega n} \triangleq [H_1(\omega) \quad H_2(\omega) \quad \cdots \quad H_M(\omega)]^T. \tag{6}$$

This representation leads to the so-called polyphase factorization

$$\boldsymbol{H}(\omega) = \boldsymbol{Q}(M\omega)\, \boldsymbol{\Delta}(\omega) \tag{7}$$

where $\boldsymbol{Q}(\omega)$ is referred to as the polyphase matrix and $\boldsymbol{\Delta}(\omega)$ is the Fourier transform of the delay chain of order M, i.e.,

$$\boldsymbol{\delta}[n] = \Big[\delta[n] \quad \delta[n-1] \quad \cdots \quad \delta[n-M+1]\Big]^T$$

when

$$\boldsymbol{\Delta}(\omega) = [1 \quad e^{-jw} \quad \cdots \quad e^{-jw(M-1)}]^T.$$

For a signature set to be orthonormal, it is necessary and sufficient that the associated polyphase matrix be paraunitary—i.e., that it satisfies, for all ω

$$\boldsymbol{Q}(\omega)\, \boldsymbol{Q}^{\dagger}(\omega) = \boldsymbol{I}. \tag{8}$$

From his perspective, choosing a signature set is equivalent to choosing a paraunitary matrix.

Several basic and widely used multiple-access strategies fit naturally within this framework. For example, the polyphase matrix corresponding to time-division multiple-access (TDMA) systems is

$$\boldsymbol{Q}(\omega) = \boldsymbol{I}$$

while that corresponding to ideal frequency-division multiple-access (FDMA) systems has (k,l)th element

$$[\boldsymbol{Q}(\omega)]_{k,l} = e^{j(w-2\pi k)l/M}, \qquad 0 \le \omega \le \pi. \tag{9}$$

In contrast, for discrete Fourier transform (DFT) based multiplexing, (which we will discuss further in the context of Section IV) $\boldsymbol{Q}(\omega)$ is the inverse of the DFT matrix, i.e.,

$$[\boldsymbol{Q}(\omega)]_{k,l} = e^{j2\pi kl/M}. \tag{10}$$

The same modulation framework can also be used to represent a variety CDMA systems that are of particular interest for use in fading environments. For example, for a direct-sequence spread spectrum CDMA system using Hadamard sequences as signatures, the polyphase matrix is

$$\boldsymbol{Q}(\omega) = \boldsymbol{\Xi} \tag{11}$$

where $\boldsymbol{\Xi}$ is the Hadamard matrix of appropriate dimension.[3]

[3]Recall that the Hadamard matrix of dimension M, viz., $\boldsymbol{\Xi}_M$, where M is a power of two, is defined recursively: for $M = 2, 4, \cdots$

$$\boldsymbol{\Xi}_M = \frac{1}{\sqrt{2}} \begin{bmatrix} \boldsymbol{\Xi}_{M/2} & \boldsymbol{\Xi}_{M/2} \\ \boldsymbol{\Xi}_{M/2} & -\boldsymbol{\Xi}_{M/2} \end{bmatrix}$$

where $\boldsymbol{\Xi}_1 = 1$.

Table 1 Nonzero Taps of the Length $N = 8$ Maximally Spread Signature Sequences in a Two User ($M = 2$) System

$n =$	0	1	2	3	4	5	6	7
$\sqrt{8}h_0[n]$	+1	+1	+1	−1	+1	+1	−1	+1
$\sqrt{8}h_1[n]$	+1	+1	+1	−1	−1	−1	+1	−1

In traditional CDMA systems like that corresponding to (11), the signature sequences $h_m[n]$ used in the modulation (2) have length equal to the intersymbol period (upsampling rate) M. In this way the signatures are used in a nonoverlapping manner for consecutive symbols of any particular user. However, we focus on the case in which the signatures have a length N that is significantly greater than M, so that signatures are used in highly lapped manner. This case is referred to as "spread-signature CDMA" [10]. Note that for such systems the polyphase matrix $\boldsymbol{Q}(\omega)$ depends explicitly on ω. More generally, for arbitrary modulation schemes $\boldsymbol{Q}(\omega)$ is independent of ω if and only if the signature set is *not* spread (i.e., $N = M$).

The key motivation for using longer signature sequence lengths N for a given symbol rate $1/M$ is that this leads to a greater temporal diversity benefit in time-varying fading.[4] In particular, the spread of a signature determines the temporal extent over which a symbol is transmitted (independent of the symbol rate). The longer this symbol duration the better the immunity to fades within the symbol interval. However, the symbol duration N cannot be chosen arbitrarily; system delay constraints generally limit the values of N that can be used in practice. From these perspectives, the best signatures in these applications have their energy spread as uniformly as possible over their length while simultaneously preserving orthogonality. When signature sequences are antipodal (i.e., $h_m[n] = \pm N^{-1/2}$), the corresponding signature sets are said to be "maximally-spread." Such signature sets are also extremely attractive in terms of computational efficiency and numerical stability.

A class of maximally spread signature sets of this type is developed and tabulated in [10] for a range of values of M and N. As an example, for $M = 2$ and $N = 8$ the nonzero taps of $h_0[n]$ and $h_1[n]$ are given in Table 1.

As discussed in [10], these signature sets are, rather interestingly, closely related to a number of orthogonal systems developed independently in a variety of other fields for wide ranging applications. For example, they are closely related to sequences constructed by Golay [14], [15], Turyn [16], Taki *et al.* [17], and Tseng and Liu [18]. Similar constructions appear in the work of both Shapiro [19] and later Rudin [20].

It is important to emphasize that these multirate systems have characteristics that are markedly different from those in source coding applications: maximally spread signature sets are localized in neither time *nor* frequency. In fact, the constituent signatures are fully broadband. As an illustration of this, Fig. 3 depicts the energy density $|H_m(\omega)|^2$ for the signature corresponding to $m = 0$ for the case $M = 2$

[4]More recently, other issues associated with the design of CDMA systems based on multirate systems have been discussed in [13].

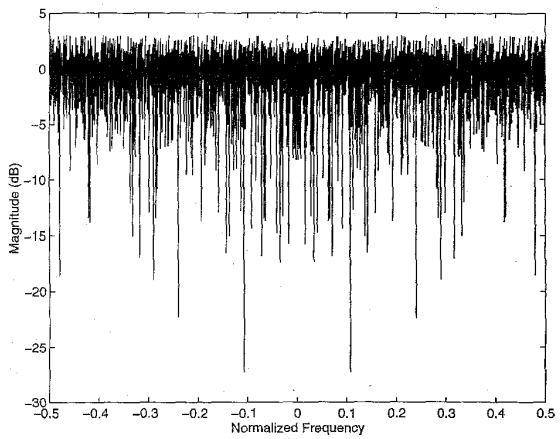

Fig. 3. Magnitude of the frequency response of the lowest filter in a spread multirate filterbank of dimension $M = 2$ and length $N = 1024$.

and $N = 1024$. Such thorough spreading in *both* time and frequency provides a highly effective form of combined temporal and spectral diversity for combating fading in wireless communication applications.

It is also worth noting that such spreading is also attractive for a range of secure communication applications, including low probability of intercept (LPI) transmission. Indeed, due to the strong overlap between signatures for consecutive symbols, the transmitted sequences $y_m[n]$ will be quasi-Gaussian even when the symbol streams $x_m[n]$ are discrete-valued. Moreover, due to the spectral characteristics of the signatures as reflected in Fig. 3, the transmitted sequences will be effectively white as well. Hence, spread-signature transmissions have characteristics much like white Gaussian noise in some important respects.

C. Spread-Signature CDMA Receivers and System Characteristics

A key feature of spread-signature CDMA is that high performance can be achieved even when relatively low complexity receivers are used. For example, in [10] a three-stage receiver is considered for recovering the mth transmitted message. The front end of this receiver is depicted in Fig. 4. First, the received data $r[n]$ is processed by a linear equalizer according to

$$\hat{y}_m[n] = \sum_k b_m[n;k]\, r[n-k] \tag{12}$$

where $b_m[n;k]$ is the kernel of the equalizer. In the second stage, the equalized data is demodulated from the corresponding signature sequence via a discrete-time matched-filter and downsample operation, viz.,

$$\hat{x}_m[n] = \sum_k \hat{y}_m[k]\, h_m[k - Mn]. \tag{13}$$

The final stage of the message recovery, which is not depicted in Fig. 4, consists of decoding the demodulated stream $\hat{x}_m[n]$ to recover the transmitted symbols.

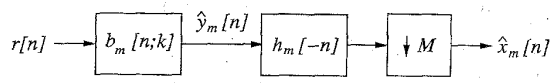

Fig. 4. Receiver structure for extracting the symbol stream of the mth user. The first stage is equalization, producing $\hat{y}_m[n]$, while the second stage is demodulation, producing $\hat{x}_m[n]$. A final stage (not shown) is decoding.

In general, the composite system consisting of modulation, the channel, equalization, and demodulation has some appealing characteristics that simplify decoding. In particular, provided the channel is ergodic and given sufficiently long signature sequences, then for a broad class of equalizers the original coded symbol stream effectively "sees" the average characteristics of the fading channel. As a consequence, the set of original coupled fading channels in the multiuser system is effectively transformed into a set of decoupled simple additive white noise channels.

More specifically, if the $x_m[n]$ is a white symbol stream then

$$\hat{x}_m[n] \approx \mu x_m[n] + v_m[n] \tag{14}$$

where the accuracy of the approximation increases with the signature length. In (14), μ is a (complex-valued) constant and the $v_m[n]$ are mutually uncorrelated, zero-mean, quasi-Gaussian white noise sequences that are uncorrelated with the streams $x_m[n]$. Furthermore, the variance of the noise $v_m[n]$ takes the form

$$\text{var}\, v_m[n] = \sigma^2_{\text{NOISE}} + \sigma^2_{\text{ISI}} + \sigma^2_{\text{MAI}}. \tag{15}$$

As (15) reflects, the equivalent noise consists of three components. The first is due the original noise $\omega[n]$ in the system after being processed by the equalizer and thus is proportional to the original noise power. The second is due to intersymbol interference (ISI), i.e., interference between the symbols in the mth user's stream that is induced by the fading process. Finally, the third term is due to multiple-access (i.e., interuser) interference (MAI) resulting from the effects of fading in the channel and asynchronism among users. Note that the ISI term is proportional to the user's transmit power and that the MAI term is proportional to a linear combination of the transmit powers of all the others users. Hence, the overall noise power in the equivalent model has a dependence on signal power, which distinguishes this channel from the usual additive white Gaussian noise channel.

As an aside, it is important to point out that in the preceding discussion the *average* transmit power of the various users are the relevant quantities in computing the equivalent noise power. In particular, the smaller the fraction of time a user is active (i.e., transmitting symbols) the smaller the corresponding average transmit power will be (for a fixed symbol energy). That reduced activity levels directly and dynamically translate into signal-to-noise/interference ratio (SNIR) enhancement is an extremely attractive feature of CDMA systems in general and spread-signature CDMA systems in particular.

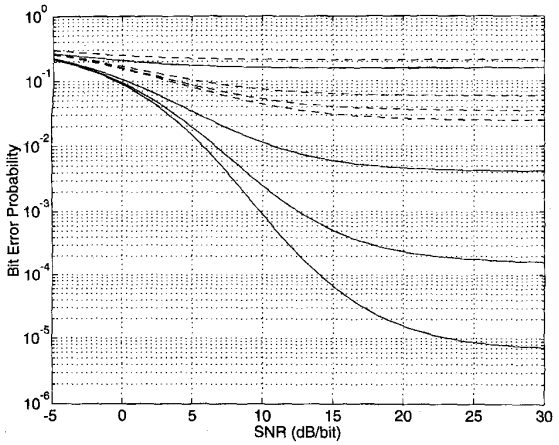

Fig. 5. Bit error probability as a function of SNR per bit for uncoded quadrature phase-shift keying (QPSK) on reverse link with infinitely many users. The successively lower solid curves correspond to the performance of spread-signature CDMA with processing gains of $\rho = 1, 7, 13, 19$. For comparison, the successively lower dashed curves correspond to the performance of conventional CDMA with the same series of processing gains.

The particular choice of equalizer has a substantial effect on the overall normalized SNIR

$$\gamma = \frac{|\mu|^2}{\sigma^2_{\text{NOISE}} + \sigma^2_{\text{ISI}} + \sigma^2_{\text{MAI}}}. \tag{16}$$

For frequency-selective slow fading channels, the SNIR (16) is maximized when the time-variant frequency response of the equalizer is [10]

$$B(\omega; n] \propto \frac{A^*_m(\omega; n]}{1 + \frac{1}{M}\sum_{k=1}^{M} \alpha_k(\omega; n]} \tag{17}$$

where $\alpha_m(\omega; n]$ is the SNR at time n and frequency ω of mth user in the original channel. It is interesting to note that with this SNIR-maximizing equalizer, $\hat{x}_m[n]$ is, coincidentally, a minimum mean-square error linear estimate of $x[n]$. In principle, this property can be exploited in implementation since it suggests that adaptive equalizers based on least-mean-square (LMS) or recursive least-squares (RLS) algorithms can be used in practice. Note, too, that the numerator of (17) is a conventional matched filter (i.e., RAKE receiver [6]), so that the denominator can be viewed as an additional compensation stage that takes into account the special characteristics of the equivalent noise in this context, as discussed earlier. Moreover, for reverse link transmission involving a large number of users, this additional compensation can generally be omitted.

The appeal of the "Rayleigh-to-Gaussian" channel transformation implied by (14) is that it suggests substantially simpler decoding algorithms can be used effectively in spread-signature CDMA receivers. In particular, from the perspective of the coded symbol stream the channel "looks" in effect like an ideal additive white Gaussian noise channel, suggesting that any of the many codes designed for this channel can be highly effective in this application. For example, if trellis coded modulation is used to generate the symbol stream, then the corresponding soft-decision Viterbi decoder that is appropriate for maximum likelihood sequence detection in additive white Gaussian noise channels can be used.

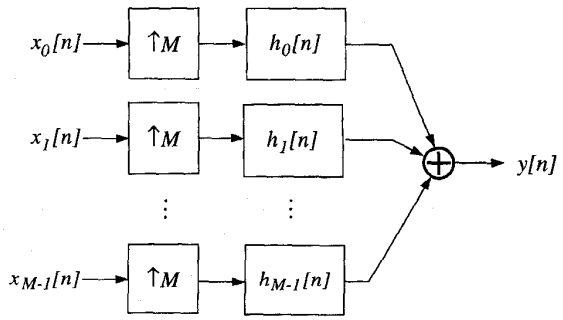

Fig. 6. Orthogonal multiplexing of substreams for single-user spread-response precoding systems.

Spread-signature CDMA systems can, in fact, be quite effective even without the use of additional coding. In this case, simple symbol-by-symbol decisions are often adequate as a decoder. As in conventional CDMA systems, excess bandwidth (beyond what is needed to support the bit rate) can be used in this scenario as a computationally inexpensive alternative to coding [10]. This bandwidth expansion translates into a spread-spectrum processing gain that boosts SNIR and, in turn, reduces bit error rate. Fig. 5 compares bit error rate for spread-signature and conventional CDMA when both are used with bandwidth expansion but no coding. The substantial advantage in using spread-signature CDMA over conventional CDMA in such specifically uncoded systems is due to the fact that the longer symbol durations in the former are much more effective at mitigating the effects of fading.

D. Single-User Systems and Spread-Response Precoding

In single-user wireless systems, spread-signature CDMA techniques lead to an efficient generalization of the "spread-response precoding" concept developed in [11] and closely related to a class of smearing techniques described by Wittneben [21].

Before proceeding, it is important to appreciate that the design of single-user systems involves some special challenges. In particular, for $M = 1$ the modulation is equivalent to prefiltering the symbol stream with a linear time-invariant (LTI) filter whose unit-sample response is the "signature sequence" $h_0[n]$. This prefiltering is referred to as spread-response precoding. In this case, the orthogonality conditions (4) and (5) are equivalent to requiring that $h_0[n]$ be an allpass filter. However, nontrivial finite-length allpass filters do not exist [22]. As a result, [11] and [21] relax the strict allpass requirement and attempt to develop quasi-orthogonal prefilters with reasonable spreading characteristics.

In such applications, substantially better performance is achieved by exploiting the orthogonal, maximally spread

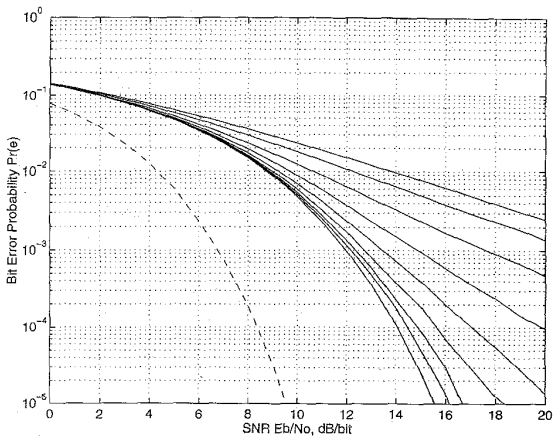

Fig. 7. Bit error probabilities using uncoded QPSK on the Rayleigh fading channel with maximally-spread precoders. The top solid curve corresponds to the performance without precoding ($N' = 1$), while the bottom solid curve indicates the performance bound corresponding to an infinite-length (delay) precoder ($N' \rightarrow \infty$). The successively lower solid curves between these two extremes represent the performance obtained using finite-spread precoders with delay parameters $N' = 2$, 4, 8, 16, 32, 64, and 128, respectively. The dashed curve is the bit error rate curve for an ideal Gaussian channel, for comparison.

systems corresponding to $M \geq 2$. This is accomplished as follows: the symbol stream $x[n]$ to be transmitted is transformed into a set of M parallel substreams

$$x_m[n] = x[\lfloor n/M \rfloor M + m] \tag{18}$$

via a serial-to-parallel converter, then these substreams are processed as if they corresponded to distinct users in a multiuser system. Specifically, the substreams are upsampled, modulated, and multiplexed as depicted in Fig. 6. In effect, this corresponds to replacing the LTI precoder with a more general linear periodically time-varying (LPTV) precoder. A suitable receiver is that described for the corresponding M-user system, and can be similarly optimized for maximum SNIR in the equivalent channel. Comparisons between the results of [11] and [10] reflect that for a given delay constraint, using maximally-spread LPTV precoders instead of LTI precoders leads to a significant reduction in bit error rate and reduces computational requirements dramatically.

Fig. 7 shows the bit error rate performance on single user fading channels using maximally-spread precoders of the type described in this section without coding. The delay constraint is expressed in terms of the normalized length N' which is a measure of the spread of the precoder relative to the coherence time of the fading.

As a final comment, it is worth emphasizing that these spread-response precoding techniques are more widely applicable for combating a variety of other channel effects as well. For example, smearing techniques have traditionally been used as a method for combating noise, interference, and jamming that is inherently impulsive in nature, and which would otherwise severely corrupt certain symbols in the transmission and leave others unaffected [23], [24].

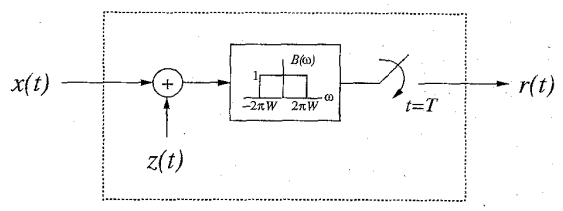

Fig. 8. Channel model for fractal modulation applications.

Spread-response precoding using maximally spread precoders constitutes an effective, computationally efficient method for mitigating the effects of these degradations as well. It is also worth noting that spread-response precoding techniques have even more distant potential applications, for example in implementing robust quantization strategies of the type developed in [25].

III. Fractal Modulation

In this section, we consider a very different channel that arises in a number of digital communications applications. As we will see, efficient linear modulation strategies based on multirate systems can also be developed for this channel. However, multirate signal processing is used in a much different way in this case. In particular, we examine a wavelet-based "fractal modulation" paradigm that has been proposed as a novel diversity strategy for communication over a particular class of unreliable channels [26], [27]. Attractively, implementations of fractal modulation make efficient use of iterated multirate filterbanks. In the following development we assume a basic familiarity with wavelet representations and multiresolution analysis; excellent introductions to these concepts can be found in [28] and [4].

A. Channel Model

The particular channel of interest has the characteristic that it is "open" for some time interval T, during which it has a particular bandwidth W and SNR. This rather basic channel model is a fairly general one for a variety of settings, and in particular it can be used to capture both characteristics of the transmission medium and constraints inherent in one or more receivers in broadcast applications. When the noise characteristics are additive, the overall channel model is as depicted in Fig. 8, where $z(t)$ represents the noise process.

When either the bandwidth or duration parameters of the channel are known *a priori* at the transmitter and receiver, there are many well-established methodologies for designing an efficient and reliable communication system. However, the focus in this section will be on the case in which *both* the bandwidth and duration parameters are either unknown or not available to the transmitter. This case, by contrast, has received comparatively less attention in the communications literature, although it arises rather naturally in a range of both point-to-point, multiple access, and broadcast communication scenarios. As one example, it can be a used in a variety jammed and meteor-burst

channels used for covert and LPI communication. As a second example, it can be used for broadcast applications in which information is being transmitted to a number of receivers having different front-end bandwidths and different processing rate capabilities.

In designing a modulation strategy for transmitting a finite-length symbol sequence $q[n]$ over such channels, it is natural to impose the following set of performance requirements:

1) Given a duration-bandwidth product $T \times W$ that exceeds some threshold, we must be able to transmit $q[n]$ without error in the absence of noise, i.e., $z(t) = 0$.
2) Given increasing duration-bandwidth product in excess of this threshold, we must be able to transmit $q[n]$ with increasing fidelity in the presence of noise. Furthermore, in the limit of infinite duration-bandwidth product, perfect transmission should be achievable at any finite SNR.

The first of these requirements implies that it must be possible to recover $q[n]$ using arbitrarily little receiver bandwidth given sufficient duration, or alternatively, from an arbitrarily short duration segment given sufficient bandwidth. The second requirement implies that it must be possible to obtain better estimates of $q[n]$ the longer a particular receiver is able to listen, or the greater the bandwidth it has available.

To meet these requirements, the modulation must contain a very special and unusual form of diversity. In particular, the system must operate efficiently over a broad range of rate-bandwidth combinations[5] using a fixed transmitter configuration, and this in turn requires that the information be embedded in the transmitted waveform on multiple time scales. A rather natural approach to achieving these objectives arises out of the concept of embedding the data to be transmitted into a homogeneous signal. Since the concept of fractal modulation is based on this idea, we briefly summarize the characteristics of homogeneous signals and describe their wavelet representations.

B. Homogeneous Signals and Wavelet Representations

A homogeneous signal $x(t)$ is a self-similar signal satisfying the deterministic scale-invariance property

$$x(t) = a^{-H} x(at) \tag{19}$$

for $a > 0$. While the set of functions satisfying (19) for all $a > 0$ is rather limited [29], a comparatively richer class of signals is obtained by requiring that (19) be satisfied only for values of a that are integer powers of two. The homogeneous signals in this broader class then satisfy the dyadic self-similarity property

$$x(t) = 2^{-kH} x(2^k t) \tag{20}$$

for all integers k. This is the class of interest for fractal modulation applications.

Homogeneous signals are inherently well suited as modulating waveforms for use on the channels described in Section III-A. Indeed, as a consequence of their intrinsic self-similarity, these waveforms have the property that an arbitrarily short duration time-segment is sufficient to recover the entire waveform, and hence the embedded information, given adequate bandwidth. Likewise an arbitrarily low-bandwidth approximation to the waveform is sufficient to recover the undistorted waveform, and again the embedded information, given adequate duration. Furthermore, homogeneous waveforms have fractal characteristics akin to those of the $1/f$ family of random processes [30].

Attractively, homogeneous signals also have efficient, wavelet-based representations that can be exploited in the development of practical systems. These representations arise out of the special relationship among wavelet coefficients for signals obeying the dyadic self-similarity property (20).

The expansion of an arbitrary signal $x(t)$ in an orthonormal wavelet basis takes the form

$$x(t) = \sum_m \sum_n x_n^m \psi_n^m(t) \tag{21a}$$

$$x_n^m = \int_{-\infty}^{+\infty} x(t) \psi_n^m(t) \tag{21b}$$

where the orthonormal wavelet basis functions are related, as usual, according to

$$\psi_n^m(t) = 2^{m/2} \psi(2^m t - n)$$

with $\psi(t)$ denoting the basic wavelet, and where m and n are the dilation and translation indexes, respectively.

When $x(t)$ is, specifically, a homogeneous signal, it follows from (21b) that the wavelet coefficients take the form

$$x_n^m = \beta^{-m/2} x_n^0 \tag{22}$$

where

$$\beta = 2^{2H+1}. \tag{23}$$

Denoting x_n^0 by $q[n]$, (21a) then becomes[6]

$$x(t) = \sum_m \sum_n \beta^{-m/2} q[n] \psi_n^m(t). \tag{24}$$

From (24) it is apparent that $x(t)$ is completely specified in terms of $q[n]$, and as a result $q[n]$ is referred to as the *generating sequence* for the homogeneous signal $x(t)$. The associated time-frequency portrait of a homogeneous signal, expressed in terms of the generating sequence, is depicted in Fig. 9. For purposes of illustration, the signal in this figure has degree $H = -1/2$ (i.e., $\beta = 1$, which corresponds to the case in which $q[n]$ is scaled by the same amplitude

[5] Note that for finite-length messages, the duration constraint T on the channel translates into a rate constraint R, and as a result it is often more natural to phrase the constraints in terms of rate-to-bandwidth ratio R/W rather than the duration-bandwidth product $T \times W$.

[6] As developed in [26], it is generally necessary to impose some mild technical restrictions on the class of wavelet bases for the representation to be well-behaved. In practice, it suffices for the wavelet $\psi(t)$ to have at least $\lceil H + 1 \rceil$ vanishing moments.

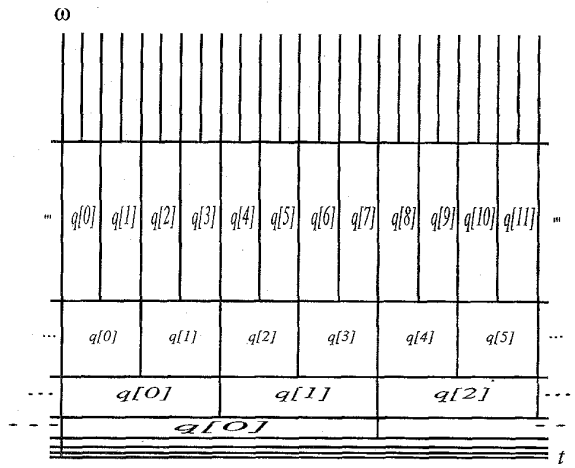

Fig. 9. The time-frequency portrait of a homogeneous signal.

factor in each octave band. The partitioning in such time-frequency portraits is of course idealized; in general, there is both spectral and temporal overlap between cells.

Homogeneous signals have several important characteristics in common with the $1/f$ family of fractal random processes. In fact, homogeneous signals can be viewed as the deterministic counterparts of $1/f$ processes, which are processes that obey the self-similarity relation (19) in a probabilistic sense. The class of $1/f$ processes are so named because they have a generalized power spectrum of the form

$$S_x(\omega) \sim \frac{1}{|w|^{2H+1}}. \tag{25}$$

Likewise, when the generating sequence $q[n]$ has finite power, the corresponding homogeneous signal also have a time-averaged power spectrum of the form (25). In addition, such homogeneous signals typically have a fractal structure similar to that of $1/f$ processes. Indeed, the Hausdorff–Besicovitch dimensions [31] of both are the same. These characteristics further the appeal of homogeneous signals as candidates for use in LPI communication applications.

However, it is important to stress that there are also important differences between homogeneous signals and $1/f$ processes. For example, a typical sample function of a $1/f$ process does not satisfy (20) but its autocorrelation function does. In turn, while the wavelet coefficients of homogeneous signals are identical from scale to scale to within an amplitude factor as (22) reflects, the wavelet coefficients of $1/f$ processes have only the same second-order statistics from scale to scale to within an amplitude factor [30]. In fact, the wavelet coefficients x_n^m from a $1/f$ process are effectively uncorrelated with the scale-to-scale variance progression

$$\text{var } x_n^m \propto \beta^{-m}.$$

1) Discrete-Time Algorithms for Homogeneous Signals: As Fig. 9 reflects, synthesizing homogeneous signals can be accomplished by replicating a generating sequence $q[n]$ at each scale in the representation (24) via an expansion in terms of an orthonormal wavelet basis. In such expansions, the detail signals in the associated multiresolution synthesis, i.e.,

$$D_m\{x(t)\} = \sum_n x_n^m \psi_n^m(t) = \beta^{-m/2} \sum_n q[n]\psi_n^m(t)$$

are simply time-dilated versions of one another, to within an amplitude factor. More generally, multiresolution synthesis leads naturally to efficient discrete-time constructions for homogeneous signals via the discrete wavelet transform (DWT). In turn, these algorithms play an important role in the development of practical communication systems based on homogeneous signals.

These algorithms arise out of a representation for a homogeneous signal in terms of what is referred to as a *characteristic sequence* $p[n]$. This sequence is defined via $p[n] = a_n^0$, where in general the coefficients a_n^m characterize the signal approximation at resolution-2^m. This approximation takes the form

$$A_m\{x(t)\} = \sum_n a_n^m \phi_n^m(t)$$

where the orthonormal basis functions are expressed in terms of the associated scaling function $\phi(t)$ according to

$$\phi_n^m(t) = 2^{m/2}\phi(2^m t - n).$$

Since the coefficients a_n^m are obtained via projections of $x(t)$ onto the $\phi_n^m(t)$, the homogeneity of $x(t)$ implies that they are identical at all scales to within an amplitude factor, i.e.,

$$a_n^m = \beta^{-m/2} a_n^0 = \beta^{-m/2} p[n]. \tag{26}$$

Hence, $p[n]$ characterizes arbitrarily fine approximations to $x(t)$, and, in turn, $x(t)$ itself.

The characteristic sequence $p[n]$ can be obtained from the generating sequence $q[n]$ via an iterative discrete-time algorithm, expressed in terms of the conjugate quadrature filter (CQF) pair associated with the wavelet basis. In particular, denoting the approximation to $p[n]$ at the ith iteration by $p^{[i]}[n]$, the algorithm is

$$p^{[0]}[n] = 0 \tag{27a}$$

$$p^{[i+1]}[n] = \beta^{1/2} \sum_k \{h[n-2k]p^{[i]}[k] + g[n-2k]q[k]\} \tag{27b}$$

where $h[n]$ and $g[n]$ are the unit sample responses of the CQF pair, i.e.,

$$h[n] = \int_{-\infty}^{+\infty} \phi_n^1(t)\phi_0^1(t)\, dt,$$

$$g[n] = \int_{-\infty}^{+\infty} \phi_n^1(t)\psi_0^1(t)\, dt.$$

This recursive upsample-filter-merge algorithm, depicted in Fig. 10, can be interpreted as repeatedly modulating $q[n]$ with the appropriate gain into successively lower octave

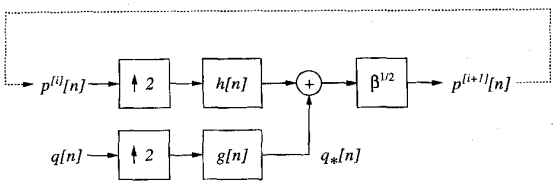

Fig. 10. Iterative algorithm for the synthesis of the characteristic sequence $p[n]$ of a homogeneous signal $x(t)$ from its generating sequence $q[n]$. The notation $p^{[i]}[n]$ denotes the value of $p[n]$ at the ith iteration.

bands of the frequency interval $0 \leq |\omega| \leq \pi$. Note that the precomputable quantity

$$q_*[n] = \sum_k g[n-2k]q[k]$$

represents the sequence $q[n]$ modulated into essentially the upper half band of frequencies.

C. Fractal Modulation Transmitter

The results of the preceding section suggest an efficient means for embedding a symbol stream $q[n]$ into a homogeneous waveform $x(t)$—in particular, it suffices to use $q[n]$ as a generating sequence for $x(t)$. This synthesis is the essence of fractal modulation, and in practice $q[n]$ is modulated into a finite number of contiguous octave-width frequency bands.

The fractal modulation transmitter can be implemented in a computationally efficient manner using the discrete-time algorithms of Section III–B1). In particular, after obtaining $p^{[M]}[n]$ from $q[n]$ using M iterations of the synthesis algorithm (27), the result is mapped into the associated continuous-time waveform by modulating with the appropriate scaling function, i.e.,

$$x(t) = \sum_n p^{[M]}[n]\phi_n^M(t) = \sum_n p^{[M]}[n]2^M\phi(2^Mt - n).$$

Finite-length messages are accommodated most efficiently by modulating their periodic extensions $q[n \bmod L]$ thereby generating a transmitted waveform

$$x(t) = \sum_m \sum_n \beta^{-m/2} q[n \bmod L]\psi_n^m(t).$$

When

$$\boldsymbol{q} = \begin{bmatrix} q[0] & q[1] & \cdots & [L-1] \end{bmatrix}$$

denotes the data vector, the time-frequency portrait associated with this signal is shown in Fig. 11. This leads naturally to a strategy for data transmission on a block-by-block basis.

The parameter H in fractal modulation controls the relative power distribution among frequency bands and, hence, the overall transmitted power spectrum, which takes the form (25). Consequently, the selection of H is important when we consider the presence of additive noise in the channel.

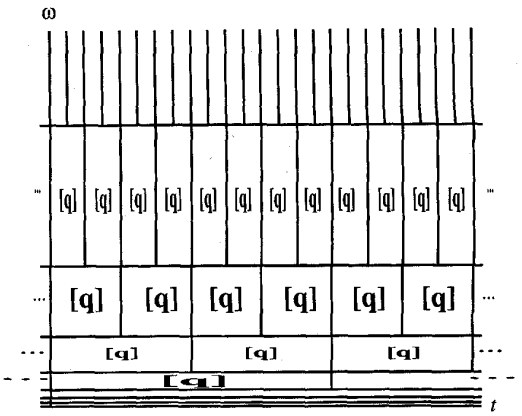

Fig. 11. A portion of the time-frequency portrait of the transmitted signal for fractal modulation of a finite-length data vector $\boldsymbol{q}$.

For traditional additive stationary Gaussian noise channels of known bandwidth, the appropriate spectral shaping of the transmitted signal is governed by a "water-pouring" procedure [32], [33], which is also the method by which the capacity of such channels is computed [1]. Using this procedure, which also plays a key role in the applications discussed in Section IV, the available signal power is distributed in such a way that proportionally more power is located at frequencies where the noise power is smaller.

When the available bandwidth is variable or unknown, which is the scenario of interest in this application, the water-pouring approach leads to poor worst-case performance. In these cases, it is preferable to distribute power according to a spectral-matching rule that maintains an SNR that is independent of frequency. This leads to a system whose performance is uniform with variations in bandwidth and, in addition, is attractive for LPI communication. Since as discussed earlier homogeneous signals and $1/f$ noises both have power spectra of the form (25), the spectral-matching rule suggests that fractal modulation may be naturally suited to channels with additive $1/f$ noise whose degree H is the same as that of the transmitted signal. Such $1/f$ noise arises in an extremely wide range of physical systems, and classical stationary white noise corresponds to the special case in which $H = -1/2$. More generally, the class of $1/f$ noises include many nonstationary noises exhibiting long-term statistical dependence among samples [30], [34].[7]

D. Fractal Modulation Receiver and Performance

For transmission of finite-length messages composed of M-ary symbols in the presence of white (or more generally $1/f$) Gaussian noise, efficient maximum likelihood (minimum probability-of-error) receivers can be developed [26]. Such receivers exploit processing in the wavelet coefficient

[7] To perform spectral matching in $1/f$ noise channels, it is typically necessary in practice to measure H based on observation of the noise process. For this purpose, the robust and efficient parameter estimation algorithms for $1/f$ processes developed in [35] and [30] can be used.

domain. Accordingly, the first stage of receiver extracts the wavelet coefficients r_n^m of the received waveform $r(t)$ using the DWT. These coefficients take the form

$$r_n^m = \beta^{-m/2} q[n \bmod L] + z_n^m \tag{28}$$

where the z_n^m are the wavelet coefficients of the noise process $z(t)$.

The duration-bandwidth characteristics of the channel in general affect which observation coefficients r_n^m may be accessed and, hence, the available redundancy. If the channel is bandlimited to 2^{M_U} Hz for some integer M_U, this precludes access to the coefficients at scales corresponding to $m > M_U$. Simultaneously, the duration-constraint in the channel results in a minimum allowable decoding rate of 2^{M_L} symbols/sec for some integer M_L, which precludes access to the coefficients at scales corresponding to $m < M_L$. As a result, the collection of coefficients available at the receiver correspond to the set of indexes

$$M_L \le m \le M_U \tag{29a}$$

$$0 \le n \le L2^{m-M_L} - 1 \tag{29b}$$

where L is the length of the message $q[n]$. This means that the available number of noisy measurements of the message is

$$K = \sum_{m=M_L}^{M_U} 2^{m-M_L} = 2^{M_U - M_L + 1} - 1. \tag{30}$$

Exploiting the fact, as discussed earlier, that the wavelet coefficients of the noise are effectively uncorrelated, a sufficient statistics for the detection of the symbol $q[n]$ is

$$\ell[n] = \sum_{m=M_L}^{M_U} \beta^{m/2} \sum_{k=0}^{2^{m-M_L}-1} r_{n+kL}^m. \tag{31}$$

Like the transmitter, the receiver has a computationally efficient, hierarchical implementation based on the DWT. With $r(t)$ bandlimited to resolution 2^{M_U}, it may be sampled at rate 2^{M_U}, then successively filtered and downsampled to level $m = M_L$ according to the usual wavelet decomposition tree. To produce the sufficient statistic $\ell[n]$, at each level m the terms from the detail sequence r_n^m corresponding to the same value of the $q[n]$ are collected together, weighted by the factor $\beta^{m/2}$, and accumulated with the weighted r_n^m from previous stages.

For binary antipodal signaling ($q[n] \in \{+\sqrt{E_0}, -\sqrt{E_0}\}$), the performance of the scheme is as depicted in Fig. 12, where bit error rate is shown as a function of the receiver rate-to-bandwidth ratio R/W and SNR. It is important to keep in mind that a receiver can select the R/W operating point dynamically since the transmitter configuration is fixed. In a broadcast application, each receiver can select its own R/W operating point and, in principle, achieve the performance reflected in Fig. 12. In this way a receiver with a slower processor speed can decode the message as reliably as one with a faster processor provided it waits longer (i.e., uses a lower rate). Or a slower processor can decode the message at the same rate as the faster processor, and accept the resulting lower fidelity in message recovery. Again, attractively, these trade-offs can be made dynamically.

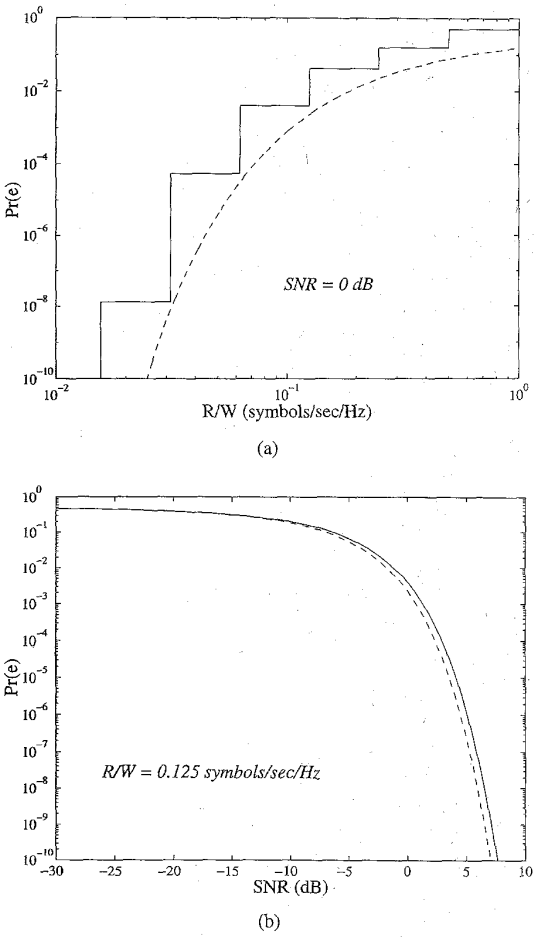

Fig. 12. Bit-error performance of fractal modulation with binary data. Solid lines indicate the performance of fractal modulation, while dashed lines indicate the performance baseline discussed in the text. (a) Bit-error probability $\Pr(e)$ as a function of rate/bandwidth ratio R/W at 0 dB SNR. (b) Bit-error probability $\Pr(e)$ as a function of SNR at $R/W = 0.125$ symbols/s/Hz.

As a baseline, Fig. 12 also shows the performance of a simple amplitude modulation scheme using time diversity in the form of repetition coding. Receivers in this system must all operate a particular common rate and bandwidth that is determined by the transmitter configuration. Hence, for this scheme different values of R/W correspond to different transmitter configurations. Further results from more extensive simulation and evaluation of fractal modulation have been described by Ptasinski and Fellman [37].

In summary, fractal modulation can be viewed as an intriguing "scale-diversity" paradigm that has potentially attractive features for data transmission in a number of secure communication and broadcast communication contexts. The essence of fractal modulation involves dividing the available transmit spectrum into multiple, adjacent, octave-spaced bands, and modulating periodic extensions of the symbol stream into these bands at the corresponding rates.

IV. Lapped Multitone Modulation

Fractal modulation can be viewed as a special form of a class of techniques broadly referred to as multitone modulation. In this section, we examine more traditional forms of multitone modulation and focus on some promising, recently proposed implementations based on efficient multirate filterbank structures. The resulting schemes can significantly enhance performance on channels that arise in a number of important emerging applications [38]. The channels of interest in this section, which we discuss next, often suffer from severe intersymbol and narrowband interference.

A. Channel Model

The equivalent discrete-time baseband model of the passband channel of interest takes the form

$$r[n] = \sum_k y[k]\, a[n-k] + w[n] \tag{32}$$

where $y[n]$ is the transmitted signal, $a[n]$ is the unit-sample response of the equivalent channel, and $w[n]$ captures both the receiver noise and other forms of interference in the system. In contrast to the scenario explored in Section II, here we consider a scenario in which both the receiver *and* the transmitter know the channel response $a[n]$, and noise and interference statistics. In applications where detailed channel characteristics are not known *a priori*, they can often be measured at the receiver and passed back to the transmitter through a feedback path. Such paths naturally exist in, e.g., a variety of two-way (full-duplex) point-to-point links.

The severe intersymbol interference (ISI) case, which is of primary interest, corresponds to a situation in which $a[n]$ has its energy dispersed over a wide temporal extent, or equivalently, in which corresponding frequency response

$$A(\omega) = \sum_n a[n]\, e^{-j\omega n}$$

exhibits large fluctuations over the frequency band. As (32) reflects, in this case each received sample $r[n]$ contains, in addition to $y[n]$, interference from a large number of neighboring samples $y[k], k \neq n$, in the transmission.

The process $w[n]$ captures both classical stationary white Gaussian receiver (thermal) noise and a variety of other forms of interference. These may include a number of narrowband interferers, so that the power spectrum of $w[n]$ contains spikes (i.e., concentrations of power) at several frequencies. Under our assumptions the receiver and transmitter have knowledge of the receiver noise power spectral density and that of the narrowband interference—specifically, the location and strength of these interferers. In addition, $w[n]$ may contain components due to crosstalk, i.e., colored interference from other poorly shielded physical communication channels in close geographic proximity [39]. Finally, $w[n]$ may contain an impulsive noise component—broadband noise that consists of short bursts of energy (clicks) randomly dispersed in time. For this component, the transmitter and receiver know the contribution of this noise to the power spectrum. However, generally the transmitter is unable to predict the actual arrival times of the clicks.

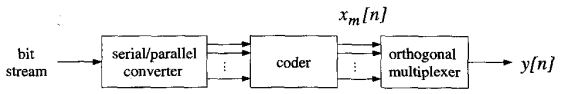

Fig. 13. A multitone system transmitter structure.

B. Applications of Multitone Modulation

Examples of channels with the kinds of characteristics described in Section IV-A and for which multitone transmission is attractive, arise in a number of important emerging applications.

One example involves asymmetric digital subscriber line (ADSL) systems. These systems have been proposed as a means for providing, among over services, video-on-demand to homes over the existing twisted pair copper wiring currently used to provide telephone service. For example, one ADSL format is designed to accommodate—in addition to the existing telephone service—the simultaneous transmission of four compressed 1.5 Mb/s video signals as well as a 384 kb/s full duplex (bidirectional) data signal. To support these data rates on a single twisted copper pair requires that very large (MHz) bandwidths be used, and even higher bandwidths are envisioned for future very high-speed digital subscriber lines (VHDSL). When used over such broad frequency ranges, twisted copper pairs exhibit many of the serious impairments included in the channel model of Section IV-A.

Another example involves proposed hybrid fiber-coax (HFC) networks—expansions of the the existing cable television (CATV) distribution network to provide additional two-way communication services [40]. These include traditional telecommunications services for voice communication, video teleconferencing, and voiceband data transmission, and well as high-speed data communication services at rates exceeding 1.5 Mb/s. In the new system, upstream transmission (i.e., from the home) will take place in the 5–40 MHz band, while downstream transmission (i.e., to the home), including television services, will take place in the 50–750 MHz band. Our channel model also captures the salient characteristics of this network. For instance, the predominant impairment in the upstream channel is severe narrowband interference referred to as "ingress" noise, which is caused by radio frequency emissions—both natural and man-made—and so-called funneling effects due to the network architecture.

Finally, the channel model of Section IV-A is a reasonable one for a variety of frequency-selective radio frequency channels whose characteristics are relatively stable (i.e., do not vary with time, or do so, at most, very slowly) [41]. Many of these channels are also subject to jamming—either unintentional or hostile—which can be captured by the narrowband interference component of the model. Furthermore, there are a number of applications of these channels

that can meet the requirement that the transmitter have access to the channel characteristics; these include, among others, point-to-point links and wireless local area networks (LAN's).

C. Communication over ISI and Colored Noise Channels

Before examining multitone modulation, we begin with some basic issues associated with designing systems for data transmission over channels of the form (32).

First, efficient communication over such channels requires a transmitted signal $y[n]$ have a suitably designed power spectrum. Specifically, as shown by Gallager [1], power must be distributed according to the general water-pouring procedure mentioned in Section III-C. With $\mathcal{E}_s$ denoting the available signal power and $S_{ww}(\omega)$ the power spectrum of the combined noise and interference, the key to this procedure involves viewing the normalized noise power density $S_{ww}(\omega)/|A(\omega)|^2$ as the bottom of a bowl into which power is "poured" until the power budget is met.

This result, which is obtained as the solution to a constrained optimization problem, corresponds to the transmitted signal $y[n]$ having a power spectrum

$$S_{yy}(\omega) = \max\left(0,\ \lambda - \frac{S_{ww}(\omega)}{|A(\omega)|^2}\right) \tag{33}$$

where the "water level" λ is a Lagrange multiplier chosen such that

$$\frac{1}{2\pi}\int_{-\pi}^{\pi} S_{yy}(\omega)\, dw = \mathcal{E}_s. \tag{34}$$

Evidently, the water-pouring algorithm will avoid allocating power to portions of the frequency spectrum where the noise or interference levels are high, such as in the vicinity of the narrowband interferers, and to portions of the spectrum where the channel is severely attenuated.

There are a variety of ways to design systems for achieving this transmit spectrum. For example, one approach begins with a basic pulse amplitude modulation (PAM) system, with or without coding, to produce an M-ary symbol stream $x[n]$. A conceptually simple method for obtaining the desired transmit spectrum for $y[n]$ involves convolving $x[n]$ with the unit-sample response $h[n]$ of a suitable LTI preemphasis filter, i.e.,

$$y[n] = x[n] * h[n].$$

Note that for the kinds of channels we have discussed, the water-pouring procedure can lead to a preemphasis filter unit-sample response $h[n]$ that is rather long. This, in turn, contributes to delay in the system.

When preemphasis filtering is used, the received signal can be expressed in the form

$$r[n] = a'[n] * x[n] + w[n] \tag{35}$$

where $a'[n]$ is the unit-sample response of the effective channel, i.e.,

$$a'[n] = a[n] * h[n].$$

For this ISI channel, maximum likelihood sequence detection can be used at the receiver to recover the transmitted symbol stream with minimum probability of error [42]. However, the computational complexity of such receivers is prohibitive in practice. Instead, more typically, the received signal is first equalized to compensate for $a'[n]$, then decoded. Linear equalization, which involves convolving $r[n]$ in (35) with a suitably chosen unit-sample response $b[n]$, is computationally attractive but generally leads to excessive noise enhancement on such channels. Instead, (nonlinear) decision feedback equalizers (DFE's) are often used. In this case, performance is further improved when the feedback portion of this receiver is implemented as Tomlinson–Harashima precoding in the transmitter [39]. With this approach, the spectral shaping is implemented as part of the (nonlinear) precoder.

The general strategy described above, when used in conjunction with trellis coded modulation, forms the basis of the current voiceband modem standard V.34 [43]. In fact, these systems can more generally achieve rates arbitrarily close to channel capacity [44], [45]. However, the voiceband modem operates over a low bandwidth channel with relatively mild impairments. For some severe intersymbol and narrowband interference channels, the multitone systems we describe next can also achieve rates arbitrarily close to capacity while at the same time offering other advantages including lower complexity implementations.

D. Multitone Modulation

Basic passband PAM as described in the previous section is sometimes referred to as a single-tone system, owing to the fact that a single carrier frequency is used with the modulation. Multitone modulation is a generalization whereby the original channel is divided into a number of orthogonal subchannels. With this system, in effect a set of PAM systems is used on separate carrier frequencies [32]. As a result, multitone modulation is also referred to as multicarrier or multichannel modulation, and sometimes orthogonal frequency division multiplexing (OFDM). Early proposed implementations of multitone modulation, such as those of Chang [46] and Saltzberg [47], were inherently continuous-time in nature. However, discrete-time implementations based on the DFT were later proposed by Weinstein and Ebert [48] and Hirosaki [49]. Now discrete-time implementations are used almost exclusively, a recent example of which is the discrete multitone transmission (DMT) system that was chosen as the ANSI T1E1.4 standard for ADSL data transmission [50].

A typical transmitter for multitone modulation is as depicted in Fig. 13. From the original bit stream, M symbol substreams $x_m[n]$ are generated via serial-to-parallel conversion and encoding, then the resulting substreams are modulated and multiplexed to obtain $y[n]$, which is transmitted as a PAM signal. The general multiplexer structure is same as that used for the spread-response precoder discussed in Section II-D and depicted in Fig. 6.

As in the case of spread-response precoding discussed in Section II-D, the discrete-time transmit pulse shapes[8] $h_m[n]$ are generally chosen to satisfy the constraints (4) and (5), so that the modulation corresponding to Fig. 6 is orthogonal. Design issues will be discussed in more detail in Section IV-G. However, we comment in advance that the factors governing the design of the $h_m[n]$ in this application are very different from those in spread-response precoding systems. In fact, as we will see, for this application it will be important that the system of Fig. 6 correspond to a multirate filter synthesis bank with good frequency localization of the type required in more traditional subband coding and time-to frequency-division transmultiplexing applications [59].

When such filters are used, an attractive feature and strong motivation for the use of multitone modulation is the comparative ease with which both transmit spectrum shaping and equalization can be often be performed. We explore these issues separately in the sections that follow.

E. Transmit Spectrum Shaping with Multitone Modulation

With multitone modulation it is comparatively easy to shape the transmit spectrum according to the water-pouring prescription dictated by capacity calculations. In effect, the available power is simply distributed among the subchannels according to a simple discretized version of the water-pouring algorithm—specifically, averages of the normalized noise power density $S_{ww}(\omega)/|A(\omega)|^2$ within each subchannel are used. Having determined the available power, the symbol sets for each subchannel are designed accordingly. For example, for uncoded systems on additive colored Gaussian noise channels, Kalet [33] described a strategy for optimizing the water-pouring and constellation design so as to obtain the minimum bit error rate subject to the constraint that this rate be the same for all subchannels that are used. More generally, coding can be used efficiently in conjunction with the modulation to achieve rates closer to capacity [51].

It is important to emphasize that with water-pouring, depending on the total available transmit power and the channel characteristics, certain subchannels may not be used at all. For example, as intuition might suggest, subchannels occupied by strong narrowband interferers are often not allocated any signal power. This provides strong motivation for using multitone systems on channels subject to this kind of interference. Indeed, to avoid excessive degradation of performance, single-tone systems used in such scenarios would require high-performance notch filtering in the transmitter to eliminate such interferers, and this filtering can be significantly more difficult to implement than the corresponding multitone system.

F. Equalization in Multitone Systems

In multitone systems, equalization can also be significantly simpler than in single-tone systems, as we now explore. The overall receiver structure we discuss is depicted in Fig. 14.

[8]To avoid potential confusion with the systems of Section II, we will avoid referring to the $h_m[n]$ as signature sequences in this application.

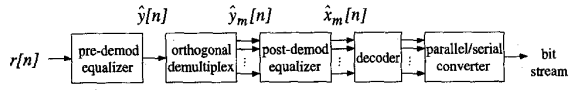

Fig. 14. A multitone system receiver structure.

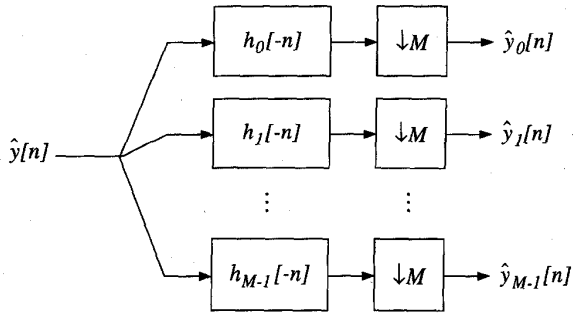

Fig. 15. The demultiplexer structure for a multitone system.

We begin by noting that because of the orthogonality of the modulation, ISI is avoided on simple additive noise channels when demultiplexing of the form depicted in Fig. 15 is used. This is the multirate filter analysis bank corresponding to the synthesis bank in Fig. 6.

When, more generally, the channel is of the form (32), then ISI interference is generally introduced. In multitone systems, this interference manifests itself in two forms. One is *interchannel* interference, which is interference between symbols being transmitted on separate subchannels—i.e., between $x_m[n]$ and $x_{m'}[n']$ for $m \neq m'$. The other is *intrachannel* interference, which is interference between different symbols being transmitted on the same subchannel—i.e., between $x_m[n]$ and $x_m[n']$ for $n \neq n'$.

When ideal bandpass filters are used, so that, consistent with (9), we have

$$H_m(\omega) = \begin{cases} \sqrt{M} & m\pi/M < |\omega| < (m+1)\pi/M \\ 0 & \text{elsewhere in } |w| < \pi \end{cases} \tag{36}$$

interchannel interference is eliminated. However, intrachannel interference remains as a consequence of the fact that the frequency response of the channel is not flat over the subchannel $m\pi/M < |\omega| < (m+1)\pi/M$. However, for channels with reasonably smooth frequency responses, frequency variations over the subchannel bandwidth are milder than over the full channel bandwidth, and thus the ISI within individual subchannels is generally substantially less severe than would be experienced using a single-tone system over the full channel bandwidth. Moreover, by increasing the number of subchannels M, this intrachannel interference can, in principle, be made arbitrarily small. However, as we will discuss shortly, other considerations generally limit values of M that can be used practice.

In some cases M can be made large enough that no additional equalization is necessary. In other cases, residual

intrachannel interference is compensated using equalization at each of the subchannel outputs $\hat{y}_m[n]$ after demultiplexing, as shown in Fig. 14. And, as also depicted in Fig. 14, in some implementations this postdemodulation equalization is combined with some predemodulation equalization applied directly to $r[n]$ [50] [38]. The role of the pre-demodulation equalizer is generally to achieve some shortening of the effective channel response, allowing simpler post-demodulation equalizers to be used in a system with a moderate numbers of subchannels M.

Of course, ideal filters of the form (36) are not realizable. In practice, finite-length filters satisfying the orthogonality constraints (4) and (5) are used, as we will discuss further in Section IV-G. For such systems, the closer the filter frequency responses are to the ideal bandpass characteristic, the lower the interchannel interference. Likewise, the shorter the filter lengths, the lower the overall system delay. However, system delay is also effectively proportional to the number of subchannels M, so that large numbers of subchannels can be impractical. As a result, a fundamental trade-off is involved: large M simplifies equalization but at the cost of delay. Moreover, the more the severe ISI (in terms of variation in the frequency response), the larger M must be to maintain a given level of performance. It should be stressed that similar tradeoffs also apply in single-tone systems, though controlling this tradeoff is often easier in multitone systems.

It is also useful to note that the longer symbol durations that result from choosing larger values of M have some significant side benefits. In particular, this temporal spreading of symbol energy is a byproduct that is useful for eliminating impulsive noise. From this perspective, such systems achieve some of the benefits of the spread-response precoding discussed in Section II-D. However, it is worth noting that when impulsive noise is the predominant channel impairment, the spread-response precoding techniques provide, in an appropriate sense, optimum immunity for a given delay. More generally, one can also control such immunity by changing the filter lengths independently of M, and in fact using spread-response techniques in conjunction with multitone systems may be useful in applications where impulsive noise is a dominant impairment.

G. Multitone Subchannel Filter Design

As in the case of spread-response and spread-signature systems, designing the frequency response vector (6) so that the overall modulation is orthogonal is equivalent to choosing a suitable paraunitary polyphase matrix $\boldsymbol{Q}(\omega)$ in (7).

Until relatively recently, most practical implementations of multitone modulation have used DFT-based multiplexing [52], [50]. For these systems, the associated polyphase matrix is given by (10), and the effective transmit pulses $h_m[n]$ are short: all have length N equal to the number of subchannels M. This property is reflected in the fact that $\boldsymbol{Q}(\omega)$ does not depend on ω for such systems. As a consequence, there is no temporal overlap between transmit pulses used to modulate symbols on a given subchannel. More specifically, there is no overlap between the pulses $h_m[n-kM]$ and $h_{m'}[n-k'M]$, which are used to modulate $x_m[k]$ and $x_{m'}[k']$, respectively, for $k \neq k'$.[9]

This absence of lapping, combined with the special structure of the DFT pulses, can facilitate equalization of finite impulse response (FIR) channels, particularly when guard bands in the form of "cyclic extensions" are used immediately following the orthogonal multiplexing in Fig. 13 [53], [52], [39]. In particular, this procedure can be used to ensure there is no ISI—either interchannel or intrachannel—in the overall multitone system, and is efficient when the channel response is shorter than the symbol duration M. On more general infinite impulse response (IIR) channels, ISI cannot be strictly eliminated through the use of such guard bands, but can be substantially reduced. In either case, the effectiveness of cyclic extensions increases with the number of subchannels M that are used.

A weakness of DFT-based multitone systems is the large spectral overlap between the frequency responses $H_m(\omega)$ of the filters corresponding to the different subchannels. In general, this can lead to substantial leakage of power between subchannels and induce significant interchannel interference. On channels with severe intersymbol and narrowband interference, systems with better spectral separation of the subchannels can offer some important advantages.

An efficient multitone system for achieving this improved spectral separation is described by Sandberg and Tzannes [38]. In their system, this separation is achieved by allowing the filters $h_m[n]$ to have lengths significantly longer than M while still preserving orthogonality. In turn, this results in the transmit pulses being used in an overlapped manner. This lapped multitone modulation concept is referred to by Sandberg and Tzannes both as "overlapped discrete multitone modulation" and discrete wavelet multitone modulation (DWMT). For these systems, efficient equalizer structures can be developed to reduce the remaining ISI [38].

Computational complexity is an important design issue for multitone systems. Indeed, an attractive feature of DFT-based multitone systems is the fact that computationally efficient implementations can be developed using the fast Fourier transform (FFT) algorithm. Similarly, in designing practical lapped multitone systems, we generally restrict attention to orthogonal multiplexers with fast algorithms. From this perspective, natural candidates for the multirate filterbanks that implement the modulation are the extended lapped transforms (ELT's) developed by Malvar [3], [54], which provide near optimal channel separation and, at the same time, have extremely efficient implementations in terms of computational complexity. The ELT is a family of orthogonal filterbanks parameterized by the overlap parameter k that determines the length of the constituent

[9] There is, however, obviously complete overlap between the effective transmit pulses of synchronous symbols in different subchannels, which is the case corresponding to $k = k'$.

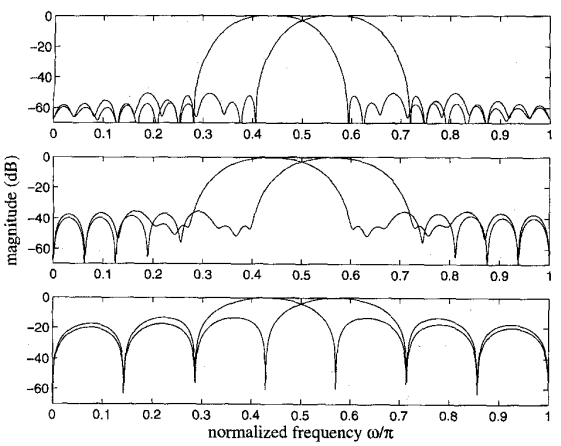

Fig. 16. Subchannel frequency response magnitudes for a pair of adjacent channels in an $M = 8$ channel multitone system. Top: lapped multitone with overlap factor of $k = 8$ symbols. Middle: lapped multitone with overlap factor of $k = 4$ symbols. Bottom: nonlapped system based on the DFT with comparable channel spacing.

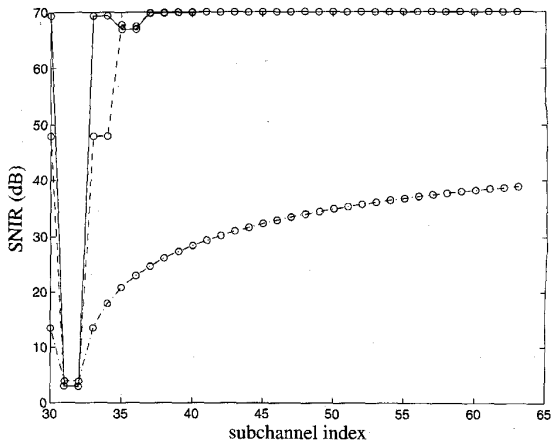

Fig. 17. SNIR levels in the subchannels of a $M = 64$ channel multitone system when a narrowband interferer is present at the center frequency of subchannel 32 and the background noise is 70 dB below this interferer. The solid and dashed curves correspond to lapped multitone with overlap factors of $k = 8$ and $k = 4$ symbols, respectively. The lower dash-dotted curve corresponds to a DFT-based nonlapped system with comparable channel spacing.

unit-sample responses; specifically, the filters have length $N = kM$.[10]

As suggested earlier, strong subchannel separation is extremely attractive from the point of view of narrowband interference rejection. Indeed, better frequency separation among the subchannels results in less leakage of narrowband interference into adjacent subchannels. Because fewer subchannels are contaminated by the interference, increased rates can be obtained.

The use of ELT's provides a convenient mechanism for trading off delay for narrowband interference rejection without changing the number of subchannels M. For example, as shown in Fig. 16, for multicarrier modulation based on DFT (i.e., DMT), the peak sidelobe is 13 dB down, while for lapped multitone modulation using ELT's, the peak sidelobe is more than 35 dB down for an overlap factor of $k = 4$ symbols, and more than 50 dB down for an overlap factor of $k = 8$ symbols. Note that typical implementations of multitone modulation use a much larger number of channels than is reflected in Fig. 16. However, systems corresponding to larger values of M exhibit similar mainlobe and sidelobe behavior.

The reduced sidelobes apparent in Fig. 16 translate into a significant improvement in narrowband interference suppression. As an illustration of this, Fig. 17 depicts how this spectral containment dramatically reduces leakage of power from a narrowband interferer into adjacent subchannels. Note that relatively few neighboring subchannels are impacted when lapped multitone modulation is used, while for nonlapped DMT systems, the interference significantly contaminates even rather distant subchannels.

H. Variations on the Multitone Theme

Our examination of multitone modulation has focused on some specific classes of these systems. However, other types of multitone systems have also attracted attention for various applications.

One example is the class of vector coding systems developed by Kasturia *et al.* [56]. These systems can be viewed as generalized nonlapped multitone modulation strategies in which the subchannel design (i.e., the $h_m[n]$) is optimized. In particular, the unitary multiplexer matrix $\boldsymbol{Q}$ is designed to partition the channel into an independent set of parallel ISI-free channels. The optimal transmit pulses shapes in this case correspond to the eigenvectors of the channel covariance matrix.[11] These optimizations are attractive from the point of view of performance, but do not necessarily lead to implementations having fast algorithms. Generalizations of vector coding to lapped multitone systems may also offer analogous advantages, and represents one of many interesting directions for further research.

Another generalization of multitone modulation is the class of nonuniform multitone systems. The subchannels of these systems do not all have the same bandwidth and therefore support different symbol rates. An example is the multitone scheme based on octave-bandwidth subchannels developed in [57]. This scheme is well suited to channels whose frequency response, noise, and interference characteristics are most naturally viewed on a logarithmic frequency scale. One example, which is explored in [57], is that where the noise process is fractal with $1/f$ spectral characteristics of the type discussed in Section III-C. More generally, the fractal modulation paradigm developed in Section III can be viewed as special case of this scheme in which a common symbol stream is transmitted in each of the subchannels to obtain a form of diversity in scale.

[10] The special case $k = 2$ also corresponds to what is also referred to as the modulated lapped transform (MLT) [55].

[11] In fact, vector coding can be viewed, in an appropriate sense, as the channel coding counterpart of the Karhunen–Loève transform in source coding.

Subchannel designs can also be obtained using other wavelet packet based structures. In turn, these may have interesting applications beyond the scope of this section. For example, versions of such systems may prove useful in frequency-hopped spread spectrum communication systems for secure transmission, or for multiple-access communications; preliminary work in the latter area is described in [58].

V. Concluding Remarks

The aim of this paper has been to provide an introduction to some promising potential applications of multirate systems, filterbanks, and wavelets in channel coding and modulation for contemporary communication systems. The development focussed on an examination of three representative examples of recently proposed techniques: spread-signature CDMA and spread-response precoding, fractal modulation, and lapped multitone modulation. Collectively, these examples suggest the tremendous breadth of emerging potential applications in the communications area.

Indeed, the continuing evolution of multirate signal processing and wavelet theory, combined with the explosive growth in the communications industry, make this a particularly fertile and timely area of research. From this perspective, it is hoped that this paper sheds some insight into some of the rich problems, interesting issues, and exciting opportunities that lie ahead. Rather than a retrospective on a mature topic, it is hoped that the paper serves as a catalyst for stimulating increased activity in a rapidly evolving area of research.

References

[1] R. G. Gallager, *Information Theory and Reliable Communication.* New York: Wiley, 1968.

[2] T. Berger, *Rate Distortion Theory: A Mathematical Basis for Data Compression.* Englewood Cliffs, NJ: Prentice-Hall, 1971.

[3] H. S. Malvar, *Signal Processing with Lapped Transforms.* Norwood, MA: Artech, 1992.

[4] M. Vetterli and J. Kovačević, *Wavelets and Subband Coding.* Englewood Cliffs, NJ: Prentice-Hall, 1995.

[5] P. P. Vaidyanathan, *Multirate Systems and Filter Banks.* Englewood Cliffs, NJ: Prentice-Hall, 1993.

[6] J. G. Proakis, *Digital Communications,* 2nd ed. New York: McGraw-Hill, 1989.

[7] W. C. Jakes, Ed., *Microwave Mobile Communications.* New York: Wiley, 1974.

[8] R. L. Pickholtz, D. L. Schilling, and L. B. Milstein, "Theory of spread-spectrum communications—a tutorial," *IEEE Trans. Commun.,* vol. COM-30, pp. 855–884, May 1982.

[9] A. J. Viterbi, *CDMA: Principles of Spread Spectrum Communication.* Reading, MA: Addison-Wesley, 1995.

[10] G. W. Wornell, "Spread-signature CDMA: Efficient multiuser communication in the presence of fading," *IEEE Trans. Inform. Theory,* vol. 41, pp. 1418–1438, Sept. 1995.

[11] ——, "Spread-response precoding for communication over fading channels," *IEEE Trans. Inform. Theory,* vol. 42, no. 2, Mar. 1996.

[12] G. W. Wornell and M. D. Trott, "Signal processing techniques for efficient use of transmit diversity in wireless communications," in *Proc. Int. Conf. Acoust. Speech, Signal Process.,* May 1996.

[13] M. K. Tsatsanis and G. B. Giannakis, "Multirate filter banks for code-division multiple access systems," in *Proc. Int. Conf. Acoust. Speech, Signal Process.,* 1995, pp. 1484–1487.

[14] M. J. E. Golay, "Multislit spectrometry," *J. Opt. Soc. Amer.,* vol. 39, pp. 437–444, 1949.

[15] ——, "Static multislit spectrometry and its application to the panoramic display of infrared spectra," *J. Opt. Soc. Amer.,* vol. 41, pp. 468–472, 1951.

[16] R. Turyn, "Ambiguity functions of complementary sequences," *IEEE Trans. Inform. Theory,* vol. IT-9, pp. 46–47, Jan. 1963.

[17] Y. Taki, H. Miyakawa, M. Hatori, and S. Namba, "Even-shift orthogonal sequences," *IEEE Trans. Inform. Theory,* vol. IT-15, pp. 295–300, Mar. 1969.

[18] C.-C. Tseng and C. L. Liu, "Complementary sets of sequences," *IEEE Trans. Inform. Theory,* vol. IT-18, pp. 644–652, Sept. 1972.

[19] H. S. Shapiro, "Extremal problems for polynomials and power series," S.M. thesis, MIT, 1951.

[20] W. Rudin, "Some theorems on Fourier coefficients," *Proc. Amer. Math. Soc.,* vol. 10, pp. 855–859, 1959.

[21] A. Wittneben, "An energy- and bandwidth-efficient data transmission system for time-selective fading channels," in *Proc. IEEE GLOBECOM,* 1990.

[22] A. V. Oppenheim and R. W. Schafer, *Discrete-Time Signal Processing.* Englewood Cliffs, NJ: Prentice-Hall, 1989.

[23] G. R. Lang, "Rotational transformation of signals," *IEEE Trans. Inform. Theory,* vol. IT-9, pp. 191–198, July 1963.

[24] G. F. M. Beenker, T. A. C. M. Claasen, and P. J. van Gerwen, "Design of smearing filters for data transmission," *IEEE Trans. Commun.,* vol. COM-33, pp. 955–963, Sept. 1985.

[25] K. Popat and K. Zeger, "Robust quantization of memoryless sources using dispersive FIR filters," *IEEE Trans. Commun.,* vol. 40, pp. 1670–1674, Nov. 1992.

[26] G. W. Wornell and A. V. Oppenheim, "Wavelet-based representations for a class of self-similar signals with application to fractal modulation," *IEEE Trans. Inform. Theory,* vol. 38, pp. 785–800, Mar. 1992.

[27] G. W. Wornell, *Signal Processing with Fractals: A Wavelet-Based Approach.* Upper Saddle River, NJ: Prentice-Hall, 1995.

[28] I. Daubechies, *Ten Lectures on Wavelets.* Philadelphia: SIAM, 1992.

[29] I. M. Gel'fand, G. E. Shilov, N. Y. Vilenkin, and M. I. Graev, *Generalized Functions.* New York: Academic, 1964.

[30] G. W. Wornell, "Wavelet-based representations for the $1/f$ family of fractal processes," *Proc. IEEE,* vol. 81, pp. 1428–1450, Oct. 1993.

[31] B. B. Mandelbrot, *The Fractal Geometry of Nature.* San Francisco: Freeman, 1982.

[32] J. A. C. Bingham, "Multicarrier modulation for data transmission: An idea whose time has come," *IEEE Commun. Mag.,* pp. 5–14, May 1990.

[33] I. Kalet, "The multitone channel," *IEEE Trans. Commun.,* vol. 37, pp. 119–124, Feb. 1989.

[34] M. S. Keshner, "$1/f$ noise," *Proc. IEEE,* vol. PROC-70, pp. 212–218, Mar. 1982.

[35] G. W. Wornell and A. V. Oppenheim, "Estimation of fractal signals from noisy measurements using wavelets," *IEEE Trans. Signal Process.,* vol. 40, pp. 611–623, Mar. 1992.

[36] H. S. Ptasinski and R. D. Fellman, "Performance analysis of a fractal modulation communication system," *Proc. SPIE,* vol. 2242, pp. 78–86, 1994.

[37] S. D. Sandberg and M. A. Tzannes, "Overlapped discrete multitone modulation for high speed copper wire communications," *IEEE J. Select. Areas Commun.,* vol. 13, pp. 1571–1585, Dec. 1995.

[38] E. A. Lee and D. G. Messerschmitt, *Digital Communication.* Boston: Kluwer, 2nd ed., 1994.

[39] R. Gross, S. Sandberg, M. Tzannes, and H. Padir, "An overview of DWMT for HFC-based telecommunications services," tech. rep., Aware, Inc., Bedford, MA, Mar. 1995.

[40] L. J. Cimini, Jr., "Analysis and simulation of a digital mobile channel using orthogonal frequency division multiplexing," *IEEE Trans. Commun.,* vol. COM-33, pp. 665–675, July 1985.

[41] G. D. Forney, Jr., "Maximum-likelihood sequence estimation of digital sequences in the presence of intersymbol interference," *IEEE Trans. Inform. Theory,* vol. IT-18, pp. 363–378, May 1972.

[42] M. V. Eyuboglu and G. D. Forney, Jr., "Trellis precoding: Combined coding, precoding, and shaping for intersymbol interference channels," *IEEE Trans. Inform. Theory,* vol. 38, pp. 301–314, Mar. 1992.

[43] J. M. Cioffi, G. P. Dudevoir, M. V. Eyuboglu, and G. D. Forney, Jr., "MMSE decision-feedback equalizers and coding—part I: Equalization results," *IEEE Trans. Commun.,* vol. 43, pp. 2582–2594, Oct. 1995.
[44] J. M. Cioffi, G. P. Dudevoir, M. V. Eyuboglu, and G. D. Forney, Jr., "MMSE decision-feedback equalizers and coding–part II: Coding results," *IEEE Trans. Commun.,* vol. 43, pp. 2595–2604, Oct. 1995.
[45] R. W. Chang, "Synthesis of band-limited orthogonal signals for multichannel data transmissions," *Bell Syst. Tech. J.,* vol. 45, pp. 1775–1796, Dec. 1966.
[46] B. R. Saltzberg, "Performance of an efficient parallel data transmission system," *IEEE Trans. Commun. Technol.,* vol. COM-15, pp. 805–811, Dec. 1967.
[47] S. B. Weinstein and P. M. Ebert, "Data transmission by frequency-division multiplexing using the discrete Fourier transform," *IEEE Trans. Commun. Technol.,* vol. COM-19, pp. 628–634, Oct. 1971.
[48] B. Hirosaki, "An orthogonally multiplexed QAM system using the discrete Fourier transform," *IEEE Trans. Commun.,* vol. COM-29, pp. 982–989, July 1981.
[49] I. Lee, J. S. Chow, and J. M. Cioffi, "Performance evaluation of a fast computation algorithm for the DMT in high-speed subscriber loop," *IEEE J. Select. Areas Commun.,* vol. 13, pp. 1564–1570, Dec. 1995.
[50] A. Ruiz, J. M. Cioffi, and S. Kasturia, "Discrete multiple tone modulation with coset coding for the spectrally shaped channel," *IEEE Trans. Commun.,* vol. 40, pp. 1012–1029, June 1992.
[51] J. S. Chow, J. C. Tu, and J. M. Cioffi, "A discrete multitone transceiver system for HDSL applications," *IEEE J. Select. Areas Commun.,* vol. 9, pp. 895–908, Aug. 1991.
[52] A. Peled and A. Ruiz, "Frequency domain data transmission using reduced computational complexity algorithms," in *Proc. Int. Conf. Acoust. Speech, Signal Process.* pp. 964–967, 1980.
[53] H. S. Malvar, "Extended lapped transforms: Properties, applications, and fast algorithms," *IEEE Trans. Signal Process.,* vol. 40, pp. 2703–2714, Nov. 1992.
[54] ——, "Lapped transforms for efficient transform/subband coding," *IEEE Trans. Acoust., Speech, Signal Process.* vol. 38, pp. 969–978, June 1990.
[55] S. Kasturia, J. T. Aslanis, and J. M. Cioffi, "Vector coding for partial response channels," *IEEE Trans. Inform. Theory,* vol. 36, pp. 741–762, July 1990.
[56] G. W. Wornell, "Communication over fractal channels," in *Proc. Int. Conf. Acoust., Speech, Signal Process.,* May 1991.
[57] R. E. Learned *et al.,* "Wavelet-packet based multiple access communication," in *Proc. SPIE on Math. Imaging,* 1994.
[58] M. Vetterli, "Perfect transmultiplexers," in *Proc. Int. Conf. Acoust. Speech, Signal Process.,* Apr. 1986, pp. 2567–2570.

Gregory W. Wornell (Member, IEEE) was born in Montréal, Canada, in 1962. He received the B.A.Sc. degree (honors) from the University of British Columbia, Canada, and the S.M. and Ph.D. degrees from the Massachusetts Institute of Technology (MIT), Cambridge, MA, all in electrical engineering, in 1985, 1987, and 1991, respectively.

Since 1991 he has been a faculty member at MIT, where he is currently ITT Career Development Assistant Professor in the Department of Electrical Engineering and Computer Science. During the 1992–1993 academic year, he was on leave at AT&T Bell Laboratories, Murray Hill, NJ, and during 1990 he was a Visiting Investigator at the Woods Hole Oceanographic Institution, Woods Hole, MA. His current research interests include signal processing, broadband and wireless communications, and applications of fractal geometry and nonlinear dynamical system theory in these areas. He is author of *Signal Processing with Fractals: A Wavelet-Based Approach* (Prentice–Hall). He holds one patent in communications and two others are pending.

Dr. Wornell held a 1967 Science and Engineering Scholarship from the Natural Sciences and Engineering Research Council of Canada from 1985 to 1989. In 1991, he received the MIT Goodwin Medal for "conspicuously effective teaching." In 1995 he received an NSF Faculty Early Career Development Award and in 1996, and ONR Young Investigator Award. He is a member of Tau Beta Pi and Sigma Xi.